Evidence of Intramolecular Regulation of the *Dictyostelium discoideum* 34 000 Da F-Actin-Bundling Protein†

Rita W. L. Lim,‡ Ruth Furukawa, and Marcus Fechheimer*

Department of Cellular Biology, University of Georgia, Athens, Georgia 30602

Received May 13, 1999; Revised Manuscript Received October 11, 1999

ABSTRACT: Intramolecular interaction within the Ca^{2+}-regulated 34 kDa actin-bundling protein from *Dictyostelium discoideum* was found to contribute to the regulation of its actin-binding activity. Recombinant N-terminally truncated proteins aa77−295, 124−295, and 139−295 bound actin at ≥2:1 stoichiometry, which is 5-fold greater than the intact protein aa1−295 as assessed by cosedimentation with F-actin. These proteins also have enhanced cross-linking activity as assessed by viscometry and electron microscopy. All truncated 34 kDa proteins failed to bind $^{45}Ca^{2+}$ on blots and displayed Ca^{2+}-insensitive binding with actin, although most proteins possessed intact putative EF-hand Ca^{2+}-binding motifs. An intramolecular interaction within the 34 kDa protein was inferred from direct demonstrations of domain−domain interaction among the truncated 34 kDa proteins both in the presence and absence of actin. The intramolecular interaction between interaction zone 1 (aa71−123) and interaction zone 2 (aa193−254) is proposed to maintain the N-terminal inhibitory region (aa1−76) in close proximity with the strong actin-binding site (aa193−254) in order to modulate the interaction of the intact protein with actin filaments.

A dynamic cytoskeleton is essential for a cell to respond to stimuli from intracellular and extracellular sources. The spatial and temporal reorganization of the cytoskeleton is brought about by the many cytoskeletal-associated proteins whose functions are often under tight regulation. In the actin-based cytoskeleton, actin-binding proteins are regulated by a variety of mechanisms. Micromolar amounts of calcium inhibit the cross-linking activity of α-actinin (*1*, *2*) and L-plastin (*3*), promote the severing activity of severin and gelsolin (*4*−*6*), and together with calmodulin aid in scruin function during the acrosomal reaction in the Limulus sperm (*7*). Several actin-binding proteins exhibit pH-sensitive activities. At pH <7.2, α-actinin, hisactophilin, ADF, and cofilin will bind actin. At pH >7.2, α-actinin and hisactophilin dissociate from actin, while ADF and cofilin depolymerize the actin filament (*1*, *8*, *9*). The phospholipid PIP_2 is known to bind profilin (*10*), cofilin (*11*), gelsolin (*12*), capping proteins (*13*), α-actinin and vinculin (*14*, *15*), and ezrin (*16*). PIP_2 can directly affect the function of the protein, for example, by enhancing actin-binding activity in α-actinin (*14*) or influencing the regulation of the protein by another mechanism such as phosphorylation (*14*, *17*−*19*). Regulation by reversible phosphorylation of myosins (*20*), actin (*21*), ADF and cofilin (*9*), and vinculin (*22*) has been documented. The focal adhesion protein vinculin and the ERM family of membrane associated actin-binding proteins, moesin, ezrin, and radixin are regulated by intramolecular interactions. Ligand-binding sites and phosphorylation sites become partially blocked or completely masked upon the head-to-tail self-association (*17*, *19*, *23*−*28*). Moreover, formation of dimers through the intermolecular association regulates the partitioning of the ERM proteins from the cytosol to specific regions of the membrane and/or the cytoskeleton (*29*−*31*).

In the cellular slime mold *Dictyostelium discoideum*, the 34 kDa actin-binding protein exhibits dynamic distributions during locomotion, phagocytosis, and development (*32*−*35*). The monomeric protein has three distinct actin-binding sites located at the regions of amino acids 1−123, 193−254, and 279−295 (*36*). The overall F-actin-binding activity of the protein is inhibited by micromolar amounts of Ca^{2+} (*32*, *37*−*39*) but is not affected by pH changes within the physiological range (*37*). Analysis of the 34 kDa protein sequence predicts two putative Ca^{2+}-binding EF-hand motifs (*40*). The regulatory mechanism of the 34 kDa protein is unknown. In this study, we present evidence of (1) an inhibitory effect of the N-terminus on the strong F-actin-binding site amino acids (aa)[1] 193−254 mapped by [^{125}I]F-actin blot overlays (*36*) and (2) an intramolecular domain−domain interaction within the 34 kDa protein. A model of the 34 kDa protein in which the intramolecular interaction folds the protein upon itself to bring the N-terminus in close proximity to inhibit the strong actin-binding site is proposed.

† Supported by NSF Grant MCB-98-08748 to R.F. and M.F. and UGA University-Wide Fellowship and Merit award to R.W.L.L..

* To whom correspondence should be addressed: Phone: (706) 542-3338. Fax: (706) 542-4271. E-mail: fechheimer@cb.uga.edu.

‡ Present address: Department of Cell Biology, The Scripps Research Institute, La Jolla, CA.

[1] Abbreviations: r34 kDa, full-length recombinant 34 kDa protein; aa, amino acids; His-βgal, histidine-tagged β-galactosidase; His-dEF1β, histidine-tagged *Dictyostelium* elongation factor 1β; GST, glutathione-*S*-transferase fusion leader protein; CAB, carbonic anhydrase; BCA, bicinchoninic acid; PBS, phosphate-buffered saline; SDS, sodium dodecyl sulfate; DTT, dithiothreitol; β-ME, β-mercaptoethanol; Pipes, piperazine-*N*,*N*′-bis(2-ethanesulfonic acid); PCR, polymerase chain reaction; IZ, interaction zone(s).

10.1021/bi991100o CCC: $18.00
Published on Web 11/16/1999

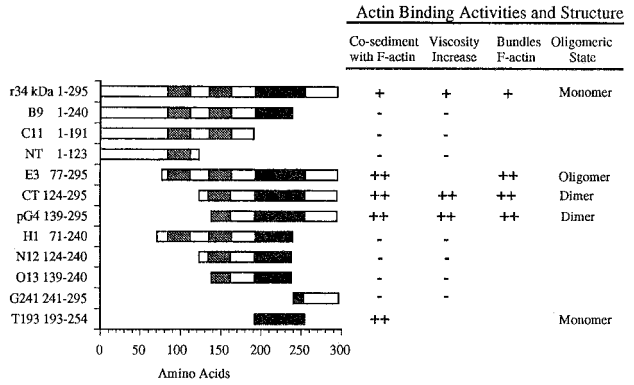

FIGURE 1: Summary of the F-actin-binding activities of the full-length and truncated 34 kDa proteins. The truncated 34 kDa proteins are denoted by the amino acid residue positions (shown on the left) corresponding to the specific regions in the full-length 295 amino acid protein. The lightly shaded boxes are putative EF-hand calcium-binding motifs, and the darkly shaded boxes are the strong actin-binding site. F-actin-binding activities were determined by high speed cosedimentation assays, low-shear falling ball viscometry, and transmission electron microscopy of negatively stained F-actin. Activity is shown as equivalent to that of the full-length 34 kDa protein (+), significantly greater than that of the intact 34 kDa protein (++), or not detectable under the described assay conditions (−).

EXPERIMENTAL PROCEDURES

Materials. His Bind resin, the pET-15b and pET-32a vectors, and AD494(DE3) bacteria were purchased from Novagen. Sephadex G-100, Sephadex G-150, gel filtration calibration standards, and the pGEX-2T vector were obtained from Pharmacia Biotech. Carbonic anhydrase (CAB), NP-40, thrombin protease, glutathione agarose, and reduced glutathione were obtained from Sigma. TALON metal affinity resin was obtained from Clontech. $^{45}CaCl_2$ was purchased from DuPont NEN. Urea (ACS grade) and Pipes buffer were purchased from Research Organics. Guanidine hydrochloride was obtained from Aldrich. BCA protein assay reagents came from Pierce. Nitrocellulose membranes (0.45 μm, BA-85) were purchased from Schleicher and Schuell.

Protein Analytical Methods. Protein concentrations were determined by the BCA method (*41*) using bovine serum albumin as the protein standard. Protein samples were analyzed on 15% SDS−PAGE (*42*), visualized by Coomassie Blue staining, and quantified by scanning densitometry (Molecular Dynamics 300A computing densitometer, Sunnyvale, CA).

Recombinant Full-Length (r34 kDa) and Truncated 34 kDa Proteins. The construction of the r34 kDa protein expression plasmid (*39*) and the truncated 34 kDa protein expression plasmids by PCR cloning of specific regions of the 34 kDa protein cDNA into pET-15b and pGEX-2T have been described (*36*). The construction of the fragment T193 (193−254) expression plasmid by subcloning the *Bgl*I/*Xho*I DNA fragment of the TvecCB/tet plasmid into pET-32a has been described (*36*). The r34 kDa protein (amino acids 1−295) (Figure 1) was expressed and purified from host bacteria BL21(DE3) as described (*39*). The truncated 34 kDa proteins, B9 (1−240), C11 (1−191), NT (1−123), E3 (77−295), CT (124−295), pG4 (139−295), H1 (71−240), N12 (124−240), and O13 (139−240) were expressed in host bacteria BL21-(DE3) and purified from the insoluble inclusion bodies using either urea or guanidine hydrochloride as described (*36*). With the exception of CT (124−295) and E3 (77−295), all the above truncated 34 kDa proteins were affinity purified on the His Bind resin under denaturing conditions with a few modifications to the manufacturer's protocol, and the histidine leader was removed by thrombin cleavage (*36*). For the affinity coprecipitation experiments where histidine-tagged truncated proteins were required to study protein interaction, the histidine leader was not removed by thrombin cleavage. The T193 (193−254) fragment was expressed in host bacteria AD494(DE3) and affinity purified from the soluble fraction on TALON beads as described (*36*). The truncated protein G241 (241−295) was expressed in host bacteria BL21 and affinity purified from the soluble fraction using glutathione agarose (*36*). The purified proteins were analyzed for their apparent native molecular weight on Sephadex G-100 (2 × 50 cm) equilibrated with 10 mM Tris-HCl, pH 7.5, 50 mM KCl, 0.1 mM EDTA, 0.02% NaN_3, and 5 mM β-ME. The gel filtration column was calibrated with cytochrome C, α-chymotrypsinogen, ovalbumin, blue dextran, and Na-ATP at a flow rate of 20 mL/h.

Actin. Sephadex G-150 column purified G-actin was prepared from rabbit skeletal muscle acetone powder (*43*, *44*) and maintained in G-actin buffer (2 mM Tris-HCl, pH 8.0, 0.2 mM $CaCl_2$, 0.2 mM ATP, 0.2 mM DTT, and 0.02% NaN_3) at 4 °C for up to 1 week with daily buffer changes. After 1 week, the G-actin was subjected to a cycle of polymerization under high salt conditions (50 mM KCl, 1 mM ATP, and 1 mM $MgCl_2$) and then depolymerization by dialysis against G-actin buffer before maintenance in G-actin buffer.

Liquid crystals of actin were prepared by polymerizing 115 μM G-actin in 20 mM Pipes, 50 mM KCl, 50 μM $MgCl_2$, and 1 mM ATP at 4 °C for 2 h (*45*). The presence of oriented domains of F-actin was confirmed visually by birefringence of polarized light transmission through dichroic sheet polarizers (Carl Zeiss Inc., Thornwood, NY) before use in attempts to mimic the conditions of the affinity cosedimentation assays.

Falling Ball Low-Shear Viscometry Assay. The viscometry assays were performed as previously described (*38*, *39*, *46*) using 4.7 μM of F-actin and increasing concentrations of the truncated 34 kDa proteins.

F-Actin High-Speed Cosedimentation Assay. Cosedimentation assays were performed as described previously (*32*, *37*, *39*). The full-length r34 kDa and truncated 34 kDa proteins (2−22 μM) were mixed with G-actin (3, 15.5, or 22 μM) under actin polymerization conditions (20 mM Pipes, pH 7.0, 50 mM KCl, 1 mM $MgCl_2$, 1 mM ATP, 5 mM EGTA, pH 7.0, and 0.2 mM $CaCl_2$ for low Ca^{2+} conditions or 4.5 mM $CaCl_2$ for high Ca^{2+} conditions) for 2 h at 4 °C and centrifuged in a Beckman airfuge at 23 psi (115000*g*) for 30 min. The supernatant (S) and the pellet (P) samples were collected and analyzed by SDS−PAGE, Coomassie Blue staining, and scanning densitometry.

Affinity Cosedimentation Assay. This method is a modification of the F-actin high-speed cosedimentation assay described above in which two different truncated 34 kDa proteins were mixed with G-actin. The full-length r34 kDa protein and the truncated 34 kDa proteins can be categorized into 2 groups on the basis of their F-actin-binding activity in the cosedimentation assays (Figure 1): (1) proteins that could cosediment with F-actin, the r34 kDa protein, fragment

T193 (193−254), and the N-terminally truncated proteins E3 (77−295), CT (124−295), and pG4 (139−295), and (2) those that failed to do so, B9 (1−240), C11 (1−191), NT (1−123), H1 (71−240), N12 (124−240), O13 (139−240), and G241 (241−295) (*36*). A concentration of 2.2−7.5 μM of two proteins, one from each category, were combined with G-actin (3, 5, or 22 μM) in the affinity cosedimentation assay. In assays where 87 μM of liquid crystalline actin was used, the category 1 protein was omitted. The assay conditions and protocols were performed as described above.

Affinity Coprecipitation Assay. Interactions among the full-length r34 kDa and truncated 34 kDa proteins were determined by affinity coprecipitation assays using histidine-tagged and GST−fusion proteins as bait. All proteins were dialyzed against buffer A (20 mM Tris-HCl, pH 8.0, 0.5 M NaCl, and 5 mM imidazole-HCl, pH 8.0) overnight at 4 °C before use in the assay. In 1.5 mL microcentrifuge tubes, 1.5 nmol of histidine-tagged or GST−fusion proteins were mixed with 1.5 nmol of nonhistidine-tagged proteins or GST−fusion protein in buffer A containing 15 mM β-ME and 0.1% NP-40 to a final volume of 550 μL. The mixture of proteins was gently agitated at room temperature for 1 h. A 25 μL aliquot of a 50% slurry of TALON metal affinity resin equilibrated with buffer A or glutathione−agarose equilibrated with PBS, pH 7.4, was added to the protein mixture, and the resin−protein mixture was mixed gently at room temperature for 15 min. The affinity resins were collected by centrifugation at 14000*g* for 30 s in a microcentrifuge, washed with 500 μL of buffer A containing 15 mM imidazole-HCl, pH 8.0 for 5 min, and collected as described above. Proteins were eluted from the TALON metal affinity resin or glutathione−agarose with 20 μL of 1 M imidazole-HCl, pH 7.9, or 10 mM reduced glutathione in 50 mM Tris-HCl, pH 8.0, respectively. The eluted proteins and the supernatant of the affinity purification containing unbound proteins were analyzed by 15% SDS−PAGE.

Calcium Binding Assay. Direct binding of calcium was determined by a modification of the $^{45}Ca^{2+}$ overlay assay (*39*, *47*). Approximately 150 pmol of the r34 kDa and truncated proteins were dot blotted onto nitrocellulose membranes. The membranes were rinsed twice in wash buffer (10 mM imidazole-HCl, pH 6.8, 60 mM KCl, and 5 mM $MgCl_2$) at room temperature for 10 min and subsequently incubated in wash buffer containing 1 μCi/mL of $^{45}Ca^{2+}$ (0.3 μM Ca^{2+}) at room temperature for 5 min. The membranes were rinsed with deionized water for 1 min, air-dried, and exposed to Kodak X-OMAT film at room temperature for 2 days.

Electron Microscopy. F-actin structures were negatively stained with 2% uranyl acetate and visualized using a Phillips 400 transmission electron microscope as previously described (*32*, *39*) with some modifications. Prepolymerized actin at 5 μM was mixed with 2 μM of the full-length r34 kDa protein or the N-terminally truncated 34 kDa proteins in polymerization buffer (20 mM Pipes, pH 7.0, 50 mM KCl, 50 μM $MgCl_2$, 0.2 mM DTT, 0.02% NaN_3, 1 mM ATP, 5 mM EGTA, and 0.2 mM $CaCl_2$) at room temperature for 2 h. The samples were applied onto 300-mesh copper grids coated with 0.3% Formvar and carbon for 30 s. The grids were rinsed with the polymerization buffer for 30 s and stained with 2% uranyl acetate for 30 s. The rinse step was omitted for the N-terminally truncated 34 kDa proteins.

RESULTS

N-Terminally Truncated 34 kDa Proteins Exhibit Enhanced F-Actin-Binding Activity. The full-length r34 kDa (1−295) protein and the N-terminally truncated 34 kDa proteins, E3 (77−295), CT (124−295), pG4 (139−295), and T193 (193−254) bound F-actin in the F-actin cosedimentation assay, while the B9 (1−240), C11 (1−191), NT (1−123), H1 (71−240), N12 (124−240), O13 (139−240), and G241 (241−295) proteins did not (Figure 1). Moreover, systematic variation of the concentration of actin and the truncated 34 kDa proteins revealed that the N-terminally truncated proteins bound F-actin more tightly than the r34 kDa protein (Figure 2A). Unbound r34 kDa protein was found in the supernatant sample when the amount of r34 kDa protein exceeded one-tenth that of actin (Figure 2A). By contrast, the truncated 34 kDa proteins pG4 (139−295), CT (124−295), and E3 (77−295) were virtually all in the pellet fraction with F-actin at concentrations not exceeding twice the concentration of F-actin (Figure 2A). Binding of the truncated 34 kDa proteins CT (124−295) and pG4 (139−295) saturated at a stoichiometry of 2 mol of truncated protein for every mole of actin (Figure 2B), while there was one r34 kDa protein bound for every two to three actin molecules under these experimental conditions (Figure 2). The binding of the truncated 34 kDa protein E3 (77−295) was somewhat higher and more variable than that of CT (124−295) and pG4 (139−295). No attempt was made to estimate the binding constants of these truncated proteins, since their binding to F-actin was essentially complete up to the point at which saturation was reached.

Gel filtration of the truncated 34 kDa proteins used in the F-actin cosedimentation assays revealed that the r34 kDa protein was a monomer, truncated proteins pG4 (139−295) and CT (124−295) proteins were dimers, and the E3 (77−295) protein contained some larger oligomers (data not shown). The E3 (77−295) and pG4 (139−295) proteins were treated with 50 mM β-ME and gel filtered in an effort to obtain monomeric proteins. However, only the pG4 (139−295) dimers could be dissociated to monomers by β-ME. The gel-filtered pG4 (gf-pG4) protein was maintained in 5 mM β-ME to prevent redimerization. When analyzed by the F-actin cosedimentation assay, the monomeric gf-pG4 protein bound to actin at a 1:1 molar ratio (Figure 2). Similarly, the T193 (193−254) protein was monomeric and bound actin at a 1:1 molar ratio (Figure 2B).

In addition, the binding of the N-terminally truncated 34 kDa proteins to F-actin in solution was not affected by micromolar amounts of calcium (data not shown), while the r34 kDa has been shown to be calcium regulated (*39*), similar to the full-length native 34 kDa protein from *D. discoideum* (*32*, *37*, *38*).

N-Terminally Truncated 34 kDa Proteins Exhibit Enhanced F-Actin Bundling Activity. Since the N-terminally truncated 34 kDa proteins bind to F-actin with higher stoichiometry than the full-length protein in the F-actin cosedimentation assay, the actin cross-linking and bundling properties of these proteins were also analyzed. The biphasic increase and decrease in the apparent viscosity of the F-actin solution in the low-shear falling ball viscometry assay is indicative of cross-linking of F-actin into an isotropic gel followed by rearrangement of the F-actin into anisotropic

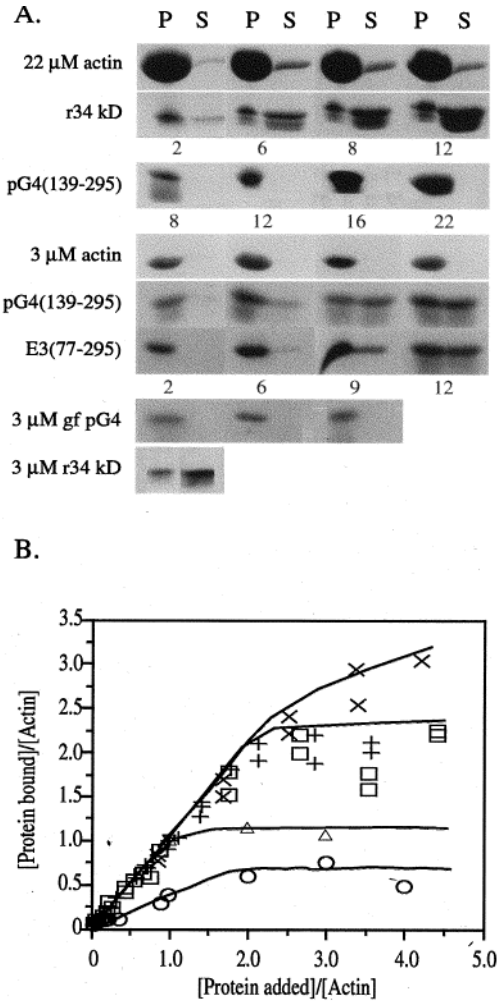

FIGURE 2: Recombinant N-terminally truncated 34 kDa proteins bind more strongly to F-actin than the full-length 34 kDa protein. (A) Coomassie Blue stained 15% SDS−PAGE gels of pellet (P) and supernatant (S) samples of F-actin cosedimentation assays conducted in the presence of 22 or 3 μM actin. Full-length recombinant 34 kDa (r34 kDa) protein and the N-terminally truncated 34 kDa proteins pG4 (139−295) and E3 (77−295) (concentration in micromolarity indicated below each panel) were mixed with 22 or 3 μM actin in the assay. Three separate preparations of Sephadex G-100 gel filtered monomeric pG4 (gf-pG4) were also assayed with 3 μM actin. Proteins remained soluble in the supernatant in the absence of actin. Proteins that bound to F-actin were found with the F-actin in the pellet. (B) Binding of the full-length and truncated r34 kDa proteins to F-actin. Data were complied from high−speed F-actin cosedimentation assays conducted at actin concentrations of 22, 15.5, and 3 μM followed by quantitative scanning densitometry of the Coomassie Blue stained 15% SDS−PAGE gels. CT (124−295) (+); E3 (77−295) (×); pG4 (139−295) (□); gf-pG4 (139−295) (▼); T193 (193−254) (△); r34 kDa protein (1−295) (○). The dimeric and monomeric N-terminally truncated proteins bound 2:1 and 1:1 to actin, respectively, while the monomeric full-length r34 kDa protein bound 1:2−3 to actin under these conditions.

bundles. Truncated 34 kDa proteins that failed to cosediment with F-actin also did not increase the apparent viscosity of the F-actin solution (Figure 1). The N-terminally truncated protein CT (124−295) increased the apparent viscosity of a 4.7 μM F-actin solution (Figure 3). The concentration at which the apparent viscosity increased sharply, the gel point, was comparable to that shown for the native *D. discoideum* 34 kDa and r34 kDa proteins (*32*, *39*). However, the F-actin gels formed by these truncated 34 kDa proteins had a lower

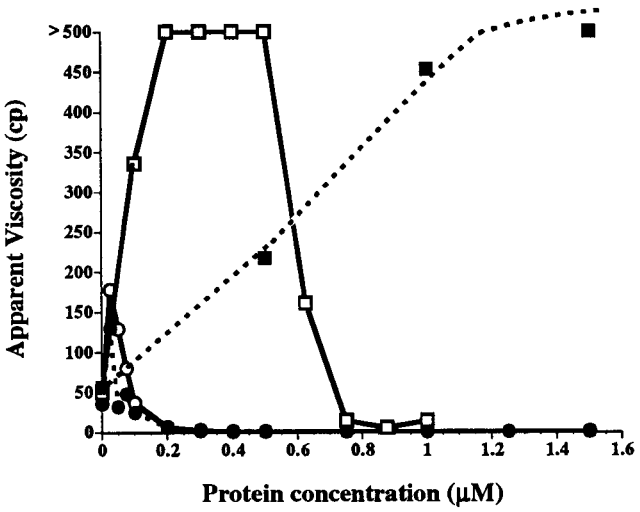

FIGURE 3: N-Terminally truncated 34 kDa protein significantly altered the apparent viscosities of F-actin solutions. Apparent viscosities of 4.7 μM F-actin in the presence of increasing amounts of the CT (124−295) protein (●, ○) and the full-length r34 kDa protein (■, □) at low calcium (5 mM EGTA:0.25 mM $CaCl_2$) condition (□, ○) and at high calcium (5 mM EGTA:4.5 mM $CaCl_2$) condition (●, ■). The F-actin gels formed with CT (124−295) were less viscous, and F-actin bundles were formed at a lower protein concentration than observed for the r34 kDa protein. Both actin gelation and bundling activities of the CT (124−295) protein were not affected by calcium, while the r34 kDa protein was significantly inhibited by calcium. Viscosity data of the r34 kDa protein was derived from ref *39*.

apparent viscosity (<200 cp) (Figure 3) than gels formed by r34 kDa protein (>500 cp) at the same protein concentrations. The apparent viscosity of the F-actin solution also decreased at lower concentrations of the truncated 34 kDa proteins (0.2 μM) (Figure 3) compared to the full-length native *D. discoideum* 34 kDa and r34 kDa proteins (>0.5 μM) (*32*, *39*), suggesting that the formation of anisotropic F-actin bundles occurred at a lower concentration of protein. The apparent viscosity of mixtures of F-actin with the dimeric pG4 (139−295) and the monomeric gf-pG4 (139−295) was similar to that obtained using the dimeric CT (124−295) (data not shown). As observed for the F-actin binding in the cosedimentation assay, both the F-actin cross-linking and bundling activities of the N-terminally truncated 34 kDa proteins, CT (124−295) (Figure 3) and pG4 (139−295) were not inhibited by calcium.

Since the viscometry data suggested that the F-actin bundling by the N-terminally truncated proteins was somewhat different from that by the full-length r34 kDa protein, the F-actin structures formed in the absence and presence of various 34 kDa proteins were studied by transmission electron microscopy. The full-length r34 kDa protein and all the N-terminally truncated proteins, E3 (77−295), CT (124−295), pG4 (139−295), and gf-pG4 (139−295), cross-linked F-actin into bundles (Figure 4, panels B−F). The F-actin bundles formed by r34 kDa protein were short, relatively straight, and thin (Figure 4B). In contrast, under identical conditions, the N-terminally truncated 34 kDa proteins made longer and thicker bundles of F-actin which were often in large tangles (Figure 4, panels C−F).

The N-terminally truncated proteins were purified from insoluble inclusion bodies and the purification protocol involved the use of protein denaturant, urea, or guanidine

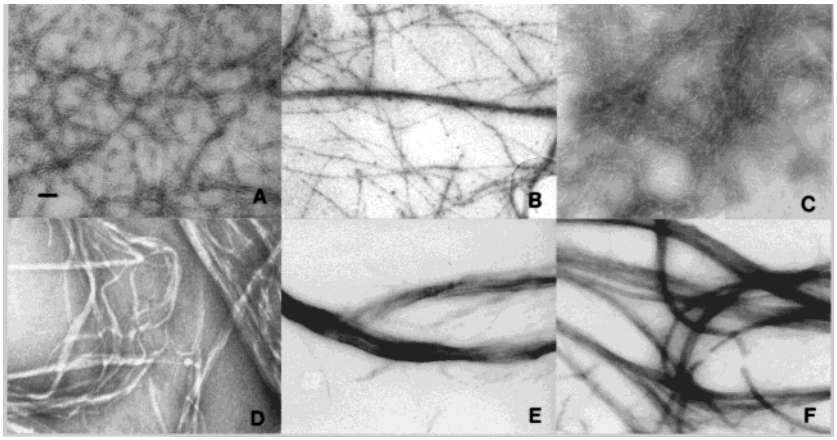

FIGURE 4: Tangles of F-actin bundles formed in the presence of N-terminally truncated 34 kDa proteins. Transmission electron micrographs of negatively stained 5 μM F-actin with or without 2 μM 34 kDa proteins. (A) F-actin only, (B) F-actin with r34 kDa protein, (C) F-actin with E3 (77−295), (D) F-actin with CT (124−295), (E) F-actin with pG4 (139−295), and (F) F-actin with monomeric gf-pG4 (139−295). Bar represents 0.05 μM.

hydrochloride. Therefore, it is conceivable that the observed increase in actin-binding activity of the N-terminally truncated 34 kDa proteins was an experimental artifact resulting from the altered conformation of the recombinant truncated proteins following protein denaturation and renaturation. To rule out this possibility, the soluble r34 kDa protein was subjected to the denaturant treatment followed by protein renaturation according to the purification procedures of the N-terminally truncated 34 kDa proteins. The urea denatured and subsequently renatured r34 kDa protein (r34U) demonstrated calcium-sensitive F-actin binding in the cosedimentation assay, and the binding was similar to the original nonurea treated r34 kDa protein (Figure 2A). Therefore, the enhanced actin-binding activity of the N-terminally truncated 34 kDa proteins is ascribed to the loss of the N-terminal region (aa 1−76), which is proposed to have an inhibitory effect on the actin-binding activity located at the C-terminus 139−295 region of the 34 kDa protein.

Domain−Domain Interactions among the Truncated Forms of the 34 kDa Protein Detected in the Presence of F-Actin. To test the hypothesis of possible intermolecular interaction among the 34 kDa truncation fragments, which would be indicative of domain−domain (i.e., intramolecular) interactions within the full-length 34 kDa protein, an affinity cosedimentation method for detecting putative interactions among truncated fragments of the 34 kDa protein was developed. The method utilizes the observation that some of the fragments such as E3 (77−295), CT (124−295), pG4 (139−295), and T193 (193−254) would cosediment with F-actin, while others such as B9 (1−240), C11 (1−191), NT (1−123), H1 (71−240), N12 (124−240), O13 (139−240), and G241 (241−295) failed to do so. The assay reveals interaction if a fragment that will not cosediment with actin does bind and pellet with filaments if mixed with another fragment that does bind F-actin directly. For example, the C11 (1−191) protein remained soluble in the supernatant during ultracentrifugation, did not cosediment with F-actin by itself, nor did it form a sedimentable complex with pG4 (139−295) alone (Figure 5A). However, in the presence of the pG4 (139−295) and F-actin, the C11 (1−191) was found completely in the pellet fraction together with pG4 (139−295) and F-actin. Control proteins of approximately similar molecular mass, the glutathione-*S*-transferase fusion leader protein (GST), and carbonic anhydrase (CAB) did not interact with pG4 (139−295) and F-actin (Figure 5, panels B and C). This shows that the phenomenon exhibits specificity and was not the result of protein entrapment by the tangles of F-actin bundles formed in the presence of the pG4 (139−

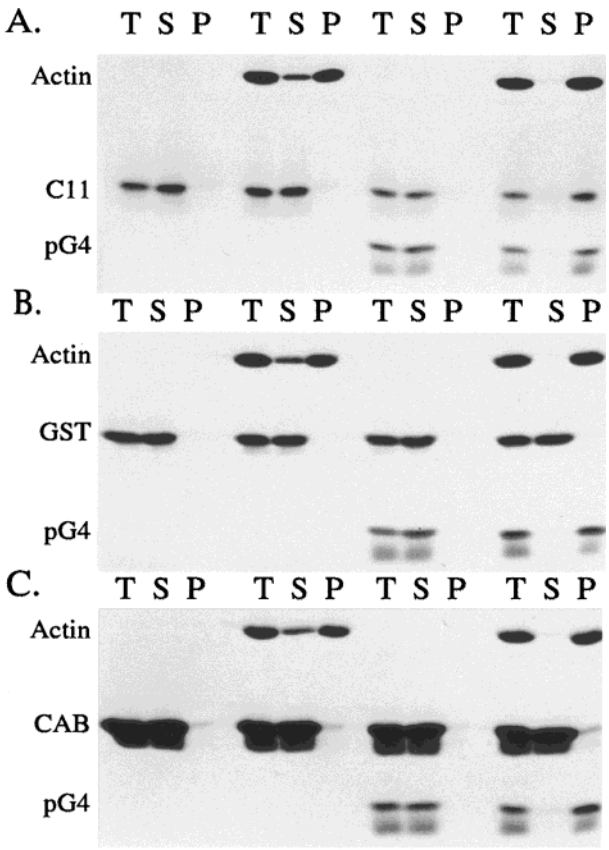

FIGURE 5: Interactions of the truncated 34 kDa proteins detected by affinity cosedimentation in the presence of actin. Coomassie Blue stained 15% SDS−PAGE gels of total (T), supernatant (S), and pellet (P) samples. (A) The strong actin-binding N-terminally truncated pG4 (139−295) (7.5 μM) and the noncosedimenting C11 (1−191) were assayed with 5 μM of actin. (B) The C11 (1−191) protein was replaced with glutathione-*S*-transferase fusion leader protein (GST). (C) The C11 (1−191) protein was replaced with carbonic anhydrase (CAB). GST and CAB served as negative controls to verify the specificity of the interaction between pG4 (139−295) and C11 (1−191). The C11 (1−191) protein was found in the pellet with F-actin only in the presence of pG4 (139−295).

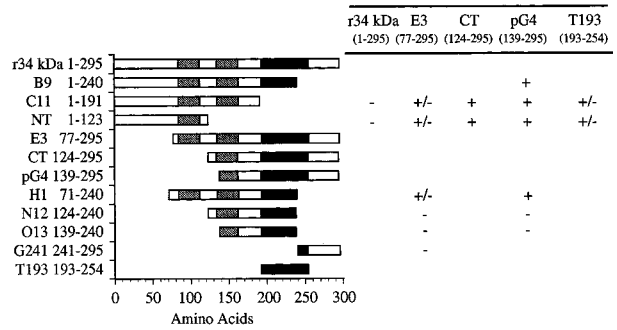

FIGURE 6: Summary of the interactions among the truncated 34 kDa proteins in the presence of actin. The truncated 34 kDa proteins are denoted by the amino acid residue positions (shown on the left) corresponding to the specific regions in the full-length 295 amino acid protein found in the truncated proteins. The lightly shaded boxes are putative EF-hand calcium-binding motifs, and darkly shaded boxes denote the strong actin-binding site. Proteins that can cosediment with actin are listed at the top, and interaction indicative of a domain−domain interaction with another truncated 34 kDa protein is indicated by the symbols. Plus (+) represents 1:1 binding for the pair of truncated 34 kDa proteins, plus/minus (±) represents a partial interaction at a lower binding ratio, and minus (−) indicates no detectable protein interaction. The minimum regions for binding mapped in this study are termed interaction zone 1 (IZ-1; aa71−123) and interaction zone 2 (IZ-2; aa193−254).

295) protein. In the presence of 5 μM actin, all 7.5 μM of the pG4 (139−295) was found in the pellet together with all 7.5 μM of C11 (1−191) (Figure 5A). The ratio of bound C11 (1−191) to pG4 (139−295) was approximately 1:1. Moreover, the increased actin-binding activity of the pG4 (139−295) was not affected by the presence of the C11 (1−191).

The studies of domain−domain interactions among the truncated forms of the 34 kDa protein detected in the presence of F-actin are summarized in Figure 6. The truncated 34 kDa proteins B9 (1−240), C11 (1−191), NT (1−123), and H1 (71−240) interact with either pG4 (139−295), CT (124−295), or E3 (77−295), while the N12 (124−240), O13 (139−240), and G241 (241−295) truncated proteins did not. The common region among those proteins that interact with pG4 (139−295), CT (124−295), and E3 (77−295) is 71−123. It was observed that the fraction of protein binding was always reduced when the E3 (77−295) was used as compared to CT (124−295) or pG4 (139−295). The smallest cosedimenting protein, T193 (193−254), would also interact and cause affinity cosedimentation of the NT (1−123) and C11 (1−191) fragments (Figure 6). Furthermore, no interaction of either the C11 (1−191) or NT (1−123) proteins with the full-length r34 kDa protein was detected in the presence of F-actin under low calcium conditions (Figure 6). In addition, all of the interactions observed by this affinity cosedimentation assay were not inhibited by calcium.

It was possible to hypothesize that the affinity cosedimentation phenomenon was due to the weak binding of the truncated 34 kDa proteins to a localized high concentration of actin found in the actin bundles rather than interaction among the truncated 34 kDa proteins. This hypothesis is plausible, since a weak actin-binding site has been localized to the N-terminus 1−123 region of the 34 kDa protein (*36*). To investigate this possibility, a simulated affinity cosedimentation assay was conducted using liquid crystals of actin

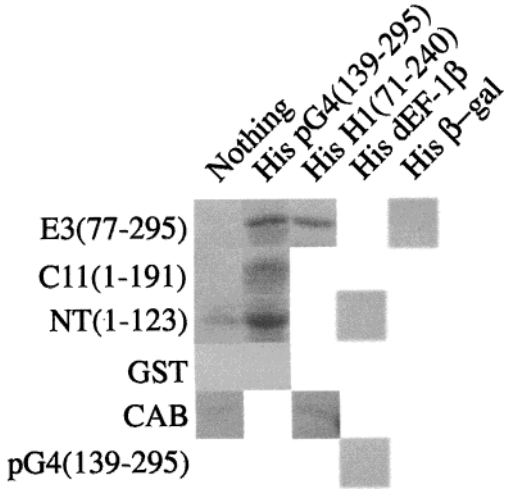

FIGURE 7: Interactions of the truncated 34 kDa proteins detected by coprecipitation in the absence of actin. Coomassie Blue stained 15% SDS−PAGE gels of proteins coprecipitating with histidine-tagged truncated 34 kDa or control proteins in affinity purification using TALON metal affinity resins. Proteins eluted from the affinity resin with 1 M imidazole, pH 7.9, are shown. Histidine-tagged β-galactosidase (His β-gal), histidine-tagged *Dictyostelium* EF1β (His dEF1-β), glutathione-*S*-transferase fusion leader protein (GST), and carbonic anhydrase (CAB) served as control proteins in the affinity coprecipitation assay. Truncated 34 kDa proteins coprecipitate specifically with tagged 34 kDa proteins.

(*45*) formed at high actin concentration to replace the pG4 (139−295) induced F-actin bundles. None of the truncated 34 kDa proteins that interact with either CT (124−295), pG4 (139−295), E3 (77−295), or T193 (193−254) were found in the pellet sample with the F-actin liquid crystals (data not shown), supporting the interpretation of specific interactions among the truncated 34 kDa proteins.

Domain−Domain Interactions among the Truncated Forms of the 34 kDa Protein Detected in the Absence of F-Actin. To affirm that there is a legitimate interaction among the truncated 34 kDa proteins, an affinity coprecipitation assay was used which did not involve actin binding. Tagged truncated 34 kDa proteins were used as bait to isolate interacting nontagged truncated 34 kDa proteins in solution. Specific interactions were observed between E3 (77−295) and His-H1 (71−240) (Figure 7) as well as His-pG4 (139−295) with NT (1−123), C11 (1−191), and E3 (77−295) (Figure 7). The nonhistidine-tagged truncated 34 kDa protein, E3 (77−295), did not coprecipitate with histidine-tagged β-galactosidase (Figure 7), nor did it bind the TALON metal affinity resin (Figure 7). Likewise, nonhistidine-tagged NT (1−123) and pG4 (139−295) did not associate with histidine-tagged *D. discoideum* EF1b (Figure 7), and the C11 (1−191) and NT (1−123) proteins did not bind the TALON resin (Figure 7). Similarly, control proteins, CAB and GST, failed to coprecipitate with the His-H1 (71−240) (Figure 7) and His-pG4 (139−295) proteins (Figure 7), respectively. The amount of coprecipitating nontagged truncated 34 kDa proteins was approximately 10−20% of the protein added in the assay.

The data obtained by the affinity coprecipitation assays using TALON metal affinity resin and glutathione agarose is summarized in Figure 8. The truncated proteins containing the regions 1−240, 1−191, 1−123, and 71−240 all interacted with the region 139−295, and the common region

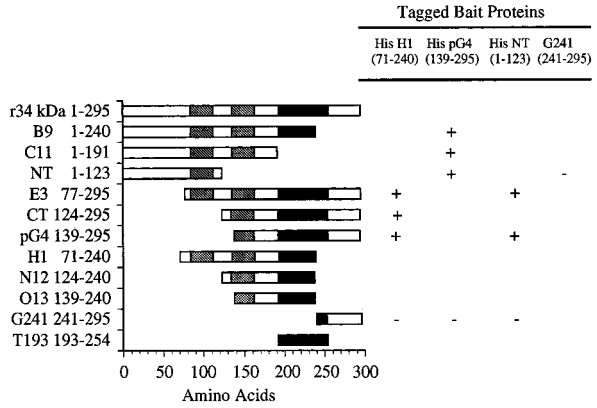

FIGURE 8: Summary of the interactions of the truncated 34 kDa proteins in the absence of actin. Data were obtained from Coomassie Blue stained 15% SDS−PAGE gels of the eluted proteins from the affinity coprecipitation assays. Histidine-tagged or GST−fusion proteins were used as bait to bind interacting truncated 34 kDa proteins, and were purified by precipitation with TALON metal affinity resin or glutathione agarose. The truncated 34 kDa proteins are denoted by the amino acid residue positions (shown on the left) corresponding to the specific regions in the full-length 295 amino acid protein found in the truncated proteins. The lightly shaded boxes are putative EF-hand calcium-binding motifs, and the darkly shaded boxes are the strong actin-binding site. All truncated 34 kDa proteins containing the common region of 71−123 would coprecipitate with any truncated 34 kDa protein with the region of 139−295.

among these four truncated proteins is 71−123. In addition, NT (1−123), H1 (71−240), and pG4 (139−295) did not coprecipitate with G241 (241−295). Combining these results with those from the affinity cosedimentation assay above (Figure 6), we deduced that the interdomain interaction regions within the 34 kDa protein are localized to the two areas, 71−123 (interaction zone 1, IZ-1) and 193−254 (interaction zone 2, IZ-2).

Direct Calcium Binding of the Truncated 34 kDa Proteins. The 34 kDa protein has been shown to bind $^{45}Ca^{2+}$ on blots, and its actin-binding activity was regulated by micromolar amounts of calcium (*32*, *37*−*39*). Since all of the actin-binding activities observed for the truncated 34 kDa protein were not affected by micromolar amounts of calcium, the ability of all the truncated 34 kDa proteins to directly bind calcium was analyzed by blot overlays. All truncated 34 kDa proteins failed to bind $^{45}Ca^{2+}$ on blots (Figure 9).

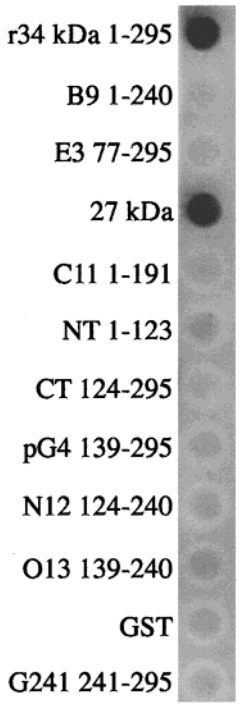

FIGURE 9: Calcium binding to the full-length and truncated 34 kDa proteins. Calcium binding was detected by autoradiography following incubation of proteins on nitrocellulose with [^{45}Ca]$CaCl_2$ as described in Materials and Methods. The full-length 34 kDa protein and 27 kDa chymotryptic fragment show calcium binding, while the truncated 34 kDa proteins do not.

DISCUSSION

In this study, we present for the first time, evidence of an intramolecular interaction which contributes to the regulation of the activity of the 34 kDa F-actin-bundling protein. The full-length 34 kDa protein has three distinct F-actin-binding sites, localized to amino acids 1−123, 193−254, and 279−295 (*36*). Truncated 34 kDa proteins containing the 1−123 or the 279−295 site alone could not cosediment with F-actin in the F-actin cosedimentation assay (*36*) (Figure 1). However, proteins that possessed the actin-binding site, 193−254, mapped by [^{125}I]F-actin blot overlays under SDS denaturing conditions (*36*), could cosediment with F-actin under high centrifugal force (Figures 1 and 2). This 62-residue sequence appears to be the strong actin-binding site, allowing the full-length r34 kDa protein and the N-terminally truncated 34 kDa proteins to cosediment with F-actin. In this study, we showed that loss of the N-terminal region (1−76) exposed greater actin-binding activity in the rest of the 34 kDa molecule. This suggests that the N-terminal region may have an inhibitory effect on the strong actin-binding site at 193−254. In addition, the putative intramolecular interaction mediating the inhibitory effect of the N-terminus has been directly demonstrated and mapped by coprecipitation experiments in both the presence and absence of F-actin.

Loss of the N-terminal region 1−76 results in extremely tight binding of the remaining C-terminal region of the 34 kDa protein to F-actin. The monomeric [gf-pG4 (139−295); T193 (193−254)] and dimeric [CT (124−295); pG4 (139−295)] amino-terminally truncated proteins exhibit a ratio of binding to actin of 1:1 and 2:1 (Figure 2), respectively, as compared to the full-length r34 kDa protein, which binds actin maximally 1:2−3 actin molecules under these experimental conditions. The amino-terminally truncated protein E3 (77−295) contains some higher oligomers and binds to F-actin at levels that exceed 2:1. The truncated proteins were also more efficient in F-actin bundle formation (Figures 3 and 4, panels C−F) forming large tangled bundles at low concentrations of cross-linking protein. The change in morphology of the bundles may be a result of the extremely tight binding of these truncated fragments to actin, as the K_d of the cross-linking protein for actin is a critical parameter in dictating the nature of the cross-linked structures that will form (*48*).

This tight actin binding was not an experimental artifact that resulted from the purification of the recombinant proteins as the urea treated and renatured r34U and the untreated r34 kDa protein exhibited similar calcium−sensitive F-actin-binding activity in the cosedimentation assays. Moreover, the 1:1 actin to 34 kDa protein-binding ratio has been reported for the bundles formed by actin and the full-length

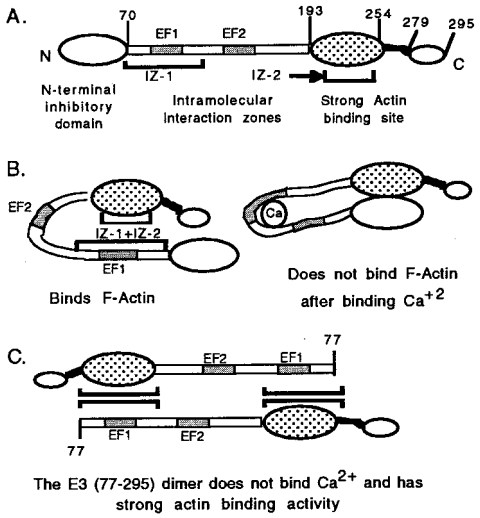

FIGURE 10: Proposed schematic model of the 34 kDa protein. (A) Extended molecule showing the structural organization of the 34 kDa protein, which includes the N-terminal inhibitory domain, the intramolecular interaction zones IZ-1 and IZ-2, the two putative EF-hand calcium-binding motifs EF1 and EF2, the strong F-actin-binding site 193−254 that was previously mapped by [^{125}I]F-actin blot overlay, and the extreme C-terminal actin-binding site 279−295 (*36*). (B) Proposed folded conformation of 34 kDa protein in the absence and presence of calcium. The intramolecular interaction between IZ-1 and IZ-2-folds the protein upon itself such that the N-terminus is brought in close proximity to the strong actin-binding site. Presumed calcium binding at the putative EF-hand(s) within the IZ-1 and/or IZ-2 results in protein conformational changes such that the N-terminus now completely blocks the strong actin-binding sites. Hence, the intact 34 kDa protein does not bind actin in the presence of calcium. (C) Model of N-terminally truncated 34 kDa protein E3 (77−295). Intermolecular interaction between IZ-1 and IZ-2 produces an antiparallel structure in which the putative EF-hands are inaccessible for calcium binding, and the strong actin-binding site 193−254 is exposed due to loss of the N-terminal inhibitory region 1−76.

native *D. discoideum* 34 kDa protein at very low actin concentrations (*49*). Hence, the intact 34 kDa protein is intrinsically capable of the greater actin-binding activity.

The presence of an intramolecular interaction within the 34 kDa protein was demonstrated in both the presence (Figures 5 and 6) and the absence (Figures 7 and 8) of actin. These results support a model of the schematic organization of the 34 kDa protein in which an intramolecular interaction within the 34 kDa protein is mediated by two regions termed interaction zone 1 (IZ-1) at 71−123 and interaction zone 2 (IZ-2) located at 193−254 (Figure 10). The intramolecular association between the IZ-1 and IZ-2 within the 34 kDa protein is proposed to maintain the N-terminal inhibitory region 1−76 in close proximity to the strong actin-binding site 193−254, thus modulating its activity in the intact protein (Figure 10B).

It is interesting to note that the inhibitory effect of the N-terminus on the actin-binding activity of the 34 kDa protein was not observed in trans between the NT (1−123) and the pG4 (139−295) proteins (Figure 6) or between the C11 (1−191) and pG4 (139−295) (Figure 5A). That is, binding of the N-terminal fragment to the C-terminal fragment did not inhibit the actin-binding activity to levels observed for the full-length 34 kDa protein. It is likely that the amino acids 124−138 that link the IZ-1 and IZ-2 in the intact molecule play a role in the proper orientation of the N-terminal inhibitory domain.

The model also proposes a plausible explanation for the effects of calcium binding on the full-length 34 kDa protein and the N-terminally truncated fragments. The intact 34 kDa protein has been shown to bind calcium and the actin-binding activities of the 34 kDa protein are inhibited by calcium (*32*, *37*−*39*). Calcium likely binds at one or both of the putative EF-hands identified in the sequence (*40*). The entire first putative EF-hand calcium-binding motif (82−112) is situated centrally within the IZ-1 (71−123), while the second EF-hand (135−163) is located adjacent to the region 193−254 which contains both the IZ-2 and the strong actin-binding site. The close spatial proximity of the IZ and the EF-hands suggests that the IZ regions could play a role in the coupling of calcium binding to inhibition of actin binding in the 34 kDa protein.

The possible effects of dimerization on the results and interpretations are crucial, since such structures could affect the actin-binding activity, avidity, and/or calcium regulation of the N-terminally truncated fragments of the 34 kDa protein. Dimers/oligomers comprise the predominant species in the preparations of the truncated recombinant proteins B9 (1−240), C11 (1−191), H1 (71−240), E3 (77−295), NT (1−123), CT (124−295), pG4 (139−295), N12 (124−240), and O13 (139−240). Yet, the structures are clearly of two distinct types. The proteins B9 (1−240), H1 (71−240), and E3 (77−295) possess the IZ-1 and IZ-2, and dimers/oligomers of these species were not dissociated by β-ME. It is likely that these more stable dimers are formed by interaction of the two IZ as shown schematically for E3 (77−295) in Figure 10C. The NT (1−123), CT (124−295), N12 (124−240), pG4 (139−295), and C11 (1−191) proteins do not contain the full IZ-1 and IZ-2 regions, and the pG4 dimers were dissociated by treatment with β-ME, indicating that they are stabilized by disulfide bridges (data not shown). We consider the properties of the fragments in light of these two types of dimeric structures.

Dimerization cannot be the primary structural basis of the increased actin binding of the truncated fragments. The monomeric form of pG4, gf-pG4, produced by reduction with β-ME and gel filtration differed from the intact 34 kDa protein and exhibited increased binding to actin and calcium insensitivity (Figure 2, 3, and 4). Similarly, the T193 (193−254) is monomeric and exhibits activated actin binding. Thus, the activating effect of the N-terminal truncation must be ascribed to removal of an inhibitory region and cannot by explained simply by dimer formation.

The E3 (77−295) oligomer is likely formed through intermolecular interaction of the IZ which results in formation of a stable complex (Figure 10C). In this conformation, the putative EF-hands may assume a conformation that differs from that in the intact 34 kDa protein in which the IZ interact intramolecularly. This could explain both the failure of the truncated 34 kDa proteins to directly bind Ca^{2+} as well as the calcium-insensitive F-actin-binding activities observed.

The difference in the structure and stability of the pG4 (139−295) dimers and E3 (77−295) oligomers also likely accounts for differences in their behavior in the affinity cosedimentation assay. The C11 (1−191), NT (1−123), and H1 (71−240) proteins all interacted less well with E3 (77−295) protein than with CT (124−295) and pG4 (139−295) (Figure 6). If the E3 (77−295) oligomer is quite stable due to intermolecular association of the IZ as proposed, then

momentary disassociation to monomer allowing redimerization with another truncated 34 kDa protein or itself would be slower than in CT (124−295) and pG4 (139−295).

The presence of the two IZ within the sequence of the 34 kDa protein suggests that the full-length protein could form multimeric species as has been observed for other proteins with intramolecular interaction zones such as vinculin (*50*) and ERM proteins (*30*, *31*, *51*). Does the full-length 34 kDa protein form dimers/oligomers through association of the IZ? Analyses of the native *D. discoideum* 34 kDa by analytical ultracentrifugation and gel filtration (*37*) indicate that the protein is a monomer in solution. Moreover, gel filtration studies performed under conditions of low and high free calcium ion concentration indicate that conformational changes associated with calcium binding involve neither formation of dimers/oligomers nor a global rearrangement between compact and extended conformations of the 34 kDa protein (*37*). However, it is possible, in theory, that the 34 kDa protein could form dimers due to a conformational change induced upon binding to actin. If dimerization did occur, truncated 34 kDa proteins containing either the IZ-1 or IZ-2 or both IZ would be expected to associate with the full-length r34 kDa protein. In vitro, this was not observed as equimolar of the NT (1−123) and C11 (1−191) protein failed to interact with the full-length r34 kDa protein (Figure 6). Thus, we conclude that the 34 kDa protein either functions as a monomeric species or forms oligomeric species that are quite unstable and short lived. A corollary is that the binding of IZ-1 to IZ-2 within the intact 34 kDa protein appears to be quite stable. If the interaction between IZ-1 and IZ-2 was not extremely stable, then 34 kDa protein molecules could freely enter an extended conformation (Figure 10A), and a profound effect of amino-terminal truncation on actin-binding activities would not have been expected. In further support of this model, point mutations within the IZ-1 produce a soluble recombinant full-length protein with strong calcium-insensitive actin-binding properties similar to those of the N-terminally truncated proteins described here (R. Furukawa, S. A. M. Thomson, R. W. L. Lim, A. Maselli, and M. Fechheimer, unpublished results). Finally, the full-length 34 kDa protein exhibits a slightly faster electrophoretic mobility following chemical cross-linking in vitro, consistent with the proposed model of the folded monomer for the intact protein (M. Fechheimer, unpublished results).

It is, nonetheless, possible that, in the cell, the 34 kDa protein does interact with other proteins, lipids, or carbohydrates and that there are cryptic ligand-binding and/or phosphorylation sites in the 34 kDa protein which could affect the intramolecular interaction between the IZ, the binding to actin, and coupling of calcium binding to the inhibition of actin binding. It is significant in this regard that membrane-associated complexes of actin and the 34 kDa protein are much less sensitive to dissociation by micromolar levels of free calcium ions than are complexes in solutions lacking membranes (*35*). The discovery of the intramolecular interaction in the 34 kDa protein suggests that binding sites for ligands other than actin might be uncovered in truncated fragments of the 34 kDa protein leading to a better understanding of the function and regulation of the protein in vivo.

Our new findings place the 34 kDa protein in a special class of cytoskeletal proteins whose functions are modulated by intramolecular interactions. Other members include the focal adhesion actin-binding protein vinculin and members of the membrane-associated actin-binding protein ERM family. The 90 kDa head domain fragment of vinculin binds α-actinin (*23*) and talin (*24*) better than the intact molecule. The C-terminus 30 kDa fragment of vinculin binds phospholipids (*26*) more tightly than the intact protein and actin-binding activity is localized to the C-terminus fragment but was not detected in the intact protein (*25*, *26*). Moreover, it was found that the head-to-tail interaction modulates the phosphorylation of vinculin (*22*). The F-actin-binding activity of ezrin, localized to the C-terminal 34 amino acids, was detected only in truncated (*27*, *52*) or SDS denatured (*28*) proteins. The head-to-tail interactions serve to partially block ligand binding and/or phosphorylation sites at the N- and C-termini and also to completely mask the C-terminus actin-binding site.

The design of the intramolecular interaction within the 34 kDa protein is somewhat different (Figure 10B). Self-association takes place between two regions, IZ-1 and IZ-2, that are arranged in tandem in the sequence of the molecule (Figure 10A). This results in the 34 kDa protein folding over upon itself such that the N-terminus is brought in close proximity to the C-terminus. The location of the two putative EF-hands in proximity to the two interaction zones allows coupling of calcium binding to regulation of actin binding as shown schematically (Figure 10B). Structural data in the form of the crystal structure of the 34 kDa protein is required to provide vital new information that will both test and refine these models for the molecular basis of the N-terminal inhibition, the intramolecular interaction, and the mechanism of calcium regulation.

ACKNOWLEDGMENT

We thank Mr. Andrew Maselli for his skillful technical assistance with the electron microscope, Mr. Tomer Tishgarten for the generous gift of the histidine-tagged *Dictyostelium* EF1β (His−dEF1β), and Mr. John Micheal Thomson for the generous gift of the histidine-tagged β-galactosidase (His−βgal). The electron microscopy was performed at the University of Georgia Center for Advanced Ultrastructure Research.

REFERENCES

1. Fechheimer, M., Brier, J., Rockwell, M., Luna, E. J., and Taylor, D. L. (1982) *Cell Motil. 2*, 287−308.
2. Brier, J., Fechheimer, M., Swanson, J., and Taylor, D. L. (1983) *J. Cell Biol. 97*, 178−185.
3. Namba, Y., M.Ito, Zu, Y., Shigesada, K., and Maruyama, K. (1992) *J. Biochem. 112*, 503−507.
4. Brown, S. S., Yamamoto, K., and Spudich, J. A. (1982) *J. Cell Biol. 93*, 205−210.
5. Yamamoto, K., Pardee, J. D., Reidler, J., Stryer, L., and Spudich, J. A. (1982) *J. Cell Biol. 95*, 711−719.
6. André, E., Lottspeich, F., Schleicher, M., and Noegel, A. (1988) *J. Biol. Chem. 263*, 722−727.
7. Sanders, M. C., Way, M., Sakai, J., and Matsudaira, P. (1996) *J. Biol. Chem. 271*, 2651−2657.
8. Scheel, J., Ziegelbauer, K., Kupke, T., Humbel, B. M., Noegel, A. A., Gerisch, G., and Schleicher, M. (1989) *J. Biol. Chem. 264*, 2832−2839.
9. Sun, H.-Q., Kwiatkowska, K., and Yin, H. L. (1995) *Curr. Opin. Cell Biol. 7*, 102−110.
10. Lassing, I., and Lindberg, U. (1985) *Nature 314*, 472−474.

11. Yonezawa, N., Homma, Y., Yahara, I., Sakai, H., and Nishida, E. (1991) *J. Biol. Chem. 266*, 17218−17221.
12. Janmey, P. A., Lamb, J., Allen, P. G., and Matsudaira, P. T. (1992) *J. Biol. Chem. 267*, 11818−11823.
13. Hartmann, H., Noegel, A. A., Eckerskorn, C., Rapp, S., and Schleicher, M. (1989) *J. Biol. Chem. 264*, 12639−12647.
14. Fukami, K., Endo, T., Imamura, M., and Takenawa, T. (1994) *J. Biol. Chem. 269*, 1518−1522.
15. Fukami, K., Sawada, N., Endo, T., and Takenawa, T. (1996) *J. Biol. Chem. 271*, 2646−2650.
16. Niggli, V., Andréoli, C., Roy, C., and Mangeat, P. (1995) *FEBS Lett. 376*, 172−176.
17. Weeks, J., Barry, S. T., and Critchley, D. R. (1996) *Biochem. J. 314*, 827−832.
18. Gilmore, A. P., and Burridge, K. (1996) *Nature 381*, 531−535.
19. Johnson, R. P., and Craig, S. W. (1995a) *Biochem. Biophys. Res. Commun. 210*, 159−164.
20. Tan, J. L., Ravid, S., and Spudich, J. A. (1992) *Annu. Rev. Biochem. 61*, 721−759.
21. Howard, P. K., Sefton, B. M., and Firtel, R. A. (1993) *Science 259*, 241−244.
22. Schwienbacher, C., Jpckusch, B. M., and Rüdiger, M. (1996) *FEBS Lett. 355*, 259−262.
23. Kroemker, M., Rüdiger, A.-H., Jockusch, B. M., and Rüdiger, M. (1994) *FEBS Lett. 355*, 259−262.
24. Johnson, R. P., and Craig, S. W. (1994) *J. Biol. Chem. 269*, 12611−12619.
25. Menkel, A. R., Kroemker, M., Bubeck, P., Ronsiek, M., Nikolai, G., and Jockusch, B. M. (1994) *J. Cell Biol. 126*, 1231−1240.
26. Johnson, R. P., and Craig, S. W. (1995) *Nature 373*, 261−264.
27. Turunen, O., Wahlström, T., and Vaheri, A. (1994) *J. Cell Biol. 126*, 1445−1453.
28. Gary, R., and Bretscher, A. (1995) *Mol. Biol. Cell 6*, 1061−1075.
29. Andréoli, C., Martin, M., LeBorgne, R., Reggio, H., and Mangeat, P. (1994) *J. Cell Sci. 107*, 2509−2521.
30. Bretscher, A., Gary, R., and Berryman, M. (1995) *Biochemistry 34*, 16830−16837.
31. Bretscher, A. (1999) *Curr. Opin. Cell Biol. 11*, 109−116.
32. Fechheimer, M. (1987) *J. Cell Biol. 104*, 1539−1551.
33. Furukawa, R., Butz, S., Fleischmann, E., and Fechheimer, M. (1992) *Protoplasma 169*, 18−27.
34. Furukawa, R., and Fechheimer, M. (1994) *Cell Motil. Cytoskeleton 29*, 46−56.
35. Fechheimer, M., Ingalls, H. M., Furukawa, R., and Luna, E. J. (1994) *J. Cell Sci. 107*, 2393−2401.
36. Lim, R. W. L., Furukawa, R., Eagle, S., Cartwright, R. C., and Fechheimer, M. (1999) *Biochemistry 38*, 800−812.
37. Fechheimer, M., and Taylor, D. L. (1984) *J. Biol. Chem. 259*, 4514−4520.
38. Fechheimer, M., and Furukawa, R. (1993) *J. Cell Biol. 120*, 1169−1176.
39. Lim, R. W. L., and Fechheimer, M. (1997) *Protein Expression Purif. 9*, 182−190.
40. Fechheimer, M., Murdock, D., Carney, M., and Glover, C. V. C. (1991) *J. Biol. Chem. 266*, 2883−2889.
41. Smith, P. K., Krohn, R. I., Hermanson, G. T., Mallia, A. K., Gartner, F. H., Provenzano, M. D., Fujimoto, E. K., Goeke, N. M., Olson, B. J., and Klenk, D. C. (1985) *Anal. Biochem. 150*, 76−85.
42. Laemmli, U. K. (1970) *Nature (London) 227*, 680−685.
43. Spudich, J. A., and Watt, S. (1971) *J. Biol. Chem. 246*, 4866−4871.
44. MacLean−Fletcher, S. D., and Pollard, T. D. (1980a) *Biochem. Biophys. Res. Commun. 96*, 18−27.
45. Furukawa, R., Kundra, R., and Fechheimer, M. (1993) *Biochemistry 32*, 12346−12352.
46. MacLean-Fletcher, S. D., and Pollard, T. D. (1980b) *J. Cell Biol. 85*, 414−428.
47. Maruyama, K., Mikawa, T., and Ebashi, S. (1984) *J. Biochem. 95*, 511−519.
48. Wachsstock, D. H., Schwatz, W. H., and Pollard, T. D. (1993) *Biophys. J. 65*, 205−214.
49. Furukawa, R., and Fechheimer, M. (1996) *Biochemistry 35*, 7224−7232.
50. Milam, L. M. (1985) *J. Mol. Biol.* 184, 543−545.
51. Berryman, M., Gary, R., and Bretscher, A. (1995) *J. Cell Biol. 131*, 1231−1242.
52. Pestonjamasp, K., Amieva, M. R., Strassel, C. P., Nauseef, W. M., Furthmayr, H., and Luna, E. J. (1995) *Mol. Biol. Cell 6*, 247−259.

BI991100O